A Matter of Life or Death: Modeling DNA Damage and Repair in Bacteria

Jens Karschau,[†] Camila de Almeida,[†‡] Morgiane C. Richard,[†‡*] Samantha Miller,[‡] Ian R. Booth,[‡] Celso Grebogi,[†] and Alessandro P. S. de Moura[†]

[†]Institute of Complex Systems and Mathematical Biology, SUPA, King's College and [‡]School of Medical Sciences, University of Aberdeen, Aberdeen, United Kingdom

ABSTRACT DNA damage is a hazard all cells must face, and evolution has created a number of mechanisms to repair damaged bases in the chromosome. Paradoxically, many of these repair mechanisms can create double-strand breaks in the DNA molecule which are fatal to the cell. This indicates that the connection between DNA repair and death is far from straightforward, and suggests that the repair mechanisms can be a double-edged sword. In this report, we formulate a mathematical model of the dynamics of DNA damage and repair, and we obtain analytical expressions for the death rate. We predict a counterintuitive relationship between survival and repair. We can discriminate between two phases: below a critical threshold in the number of repair enzymes, the half-life decreases with the number of repair enzymes, but becomes independent of the number of repair enzymes above the threshold. We are able to predict quantitatively the dependence of the death rate on the damage rate and other relevant parameters. We verify our analytical results by simulating the stochastic dynamics of DNA damage and repair. Finally, we also perform an experiment with *Escherichia coli* cells to test one of the predictions of our model.

INTRODUCTION

DNA in living cells is constantly subject to attack from various agents, ranging from ultraviolet light and ionizing radiation to toxic chemical species (1). The damaging agents may come from the environment, but they may also be endogenous, produced by the cell's own metabolism (2). The action of many of these agents is to cause anomalous changes in chemical bonds of nucleotides, resulting in damaged bases in the DNA. In many situations, single bases are damaged in each damaging event, giving rise to a single base damage. The damaged bases compromise the transcription and replication machines of the cell, thus affecting its viability (3). Because of the ubiquity and potentially deadly consequences of single base DNA damages, organisms have evolved various mechanisms for repairing them (3,4).

Although the details vary from organism to organism, the modus operandi of most single base repair mechanisms is very similar. First, the damaged site is identified by the appropriate enzyme; then, in a concerted action enacted by a series of enzymes, a region of the DNA strand containing the damaged base is excised. Subsequently the missing piece is resynthesized, using the opposite strand as a template; a ligase finishes the job by sealing the newly formed oligonucleotide to the rest of the DNA strand (1,5,6). The precise biochemical processes involved in single base repair depend on the repair mechanism. In nucleotide excision repair, for instance, the damaged base is recognized by the association of the enzymatic complex formed by UvrA, UvrB, and ATP, and a region ~10 bases long around the damaged site is removed by the enzyme complex UvrB-UvrC; DNA polymerase and DNA ligase then rebuilds the exposed single strand sequence (5,6).

Another repair mechanism is base excision repair, during which damage is recognized by N-glycosylases. In this mechanism, the DNA molecule is nicked by an exonuclease enzyme near the damaged base, and then the neighboring bases in the same strand are successively discarded and new bases added by DNA polymerase; finally, DNA ligase connects the newly formed sequence to the original strand (5).

One crucial feature of both repair mechanisms described above, and of all excision damage repair schemes, is that while the repair is taking place, one section of the DNA molecule becomes single-stranded. If there is another damaged base on the opposite strand and close enough to a base which is currently being repaired, then repair may start at this other base before the repair on the opposite base has been completed; the result is the creation of a double-strand break (DSB), which breaks apart the DNA molecule (7). DSBs are frequently fatal to cells (1,8–10). Thus, the excision repair mechanism itself is largely responsible for killing cells subject to DNA damage. This fact is of the utmost importance for properly understanding the dynamics of this process, and it is often forgotten in mathematical models of mortality resulting from DNA damage (11–17).

A good mathematical model of the dynamics of DSB formation in DNA damage and repair is essential to understand quantitatively the relation between the mortality rate and the concentration of damaging agents. In this article, we focus on endogenous DNA damaging agents, which is a common situation bacteria face in their life cycle (18,19). We use as our example system *Escherichia coli* (*E. coli*) bacteria exposed to the electrophile methylglyoxal (MG).

Submitted September 1, 2010, and accepted for publication December 15, 2010.

*Correspondence: m.richard@abdn.ac.uk

Camila de Almeida's present address is AstraZeneca, Mereside, Alderley Park, Macclesfield, Cheshire SK104TG, UK.

Editor: Leslie M. Loew.

0006-3495/11/02/0814/8 $2.00

doi: 10.1016/j.bpj.2010.12.3713

E. coli produces MG under conditions of unbalanced sugar metabolism (19,20). MG primarily attacks the guanine bases of the DNA (2,21), which are repaired by the excision mechanism (18). We formulate a mathematical model of the dynamics of damage and repair processes taking place in the presence of a damaging agent such as MG, and we assume that DSBs are 100% lethal and that they are the only cause of death. In other words, we identify the death rate with the rate of creation of DSBs during repair.

We are interested primarily in how the rate of creation of DSBs by the repair mechanism depends on the concentration of MG (or other relevant damaging agent) and on the abundance of repair enzymes in cells. We show that the dynamics of DSB creation has two very different regimes, depending on the number N_E of repair enzymes present in the cell: if N_E is greater than a critical value N_c, the rate of DSB formation R increases quadratically with the concentration M of the toxin, and is independent of N_E; if, on the other hand, $N_E < N_c$, R is independent of M, and increases with N_E. These are counterintuitive predictions, which challenge the usual assumptions made about the dynamics of the repair process; in particular, the death rate can actually increase with the number of repair enzymes. These surprising results are direct consequences of the fact that cell death is caused by repair-induced DSBs, and not directly by DNA damage itself. We obtain analytical results from our model, checked and complemented by stochastic numeric simulations. We also perform an experiment to measure the mortality rate of *E. coli* bacteria exposed to methylglyoxal, and compared the results to our model predictions; we find that the results compare well with the theory.

METHODS

Model assumptions

The prime objective of the mathematical model we present here is to predict the death rate of microorganisms as a result of creation of DSBs during repair of DNA damage caused by harmful chemical agents such as the electrophile MG. Although we use *E. coli* as the model organism, we expect our approach and many of our results to apply to other organisms, because both DNA damage and repair processes are well conserved across species (5,6). The following assumptions are taken in the model described in this work:

1. The definition of death is often a controversial issue, because cellular death is usually not instantaneous and can be characterized by a variety of biochemical events (22,23). Here we adopt the simplified view that cell death coincides with the appearance of double-strand breaks in the chromosome during repair, as described in the Introduction (10,24,25).
2. We use experimental conditions which ensure that cell growth is inhibited (20), therefore we consider that the cell volume is constant. We assume that the concentration, and consequently, the total number of repair enzymes is constant.
3. Enzymes can be either free or bound to a damaged site. Only free enzymes may be engaged in a repair, and once repair is finished, bound enzymes are freed again. This is crucial in modeling DNA repair, because the number of repair enzymes found in wild-type cells is expected to be very low (26–31).
4. Although many different enzymes are involved in the repair mechanisms, repair is always initiated by a sensor enzyme which detects damage (1,5,6). In nucleotide excision repair, for example, this is the *UvrA* enzyme. We will focus on these sensor enzymes, and the four steps described in the Introduction (identification, excision, synthesis, and ligation) will be subsumed in a single parameter, the single base repair rate.
5. Double-strand breaks appear when two repairs take place simultaneously at opposite strands, and are sufficiently close to each other. We will model this phenomenon by assuming that, if repair starts at a damaged base lying within some fatal distance from another damaged base being repaired on the opposite strand, a double-strand break results. The fatal distance is ~10 bases (6).
6. In the situation we are mostly interested in here, new damaged sites are constantly being created by the action of the toxin, at a rate proportional to its concentration within the cell (32). Methylglyoxal attacks guanine preferentially, and other chemicals may be reactive with different nucleotides (2,21). We assume that the affected bases are homogeneously distributed in the chromosome, and so bases are damaged randomly with uniform probability throughout the length of the chromosome.
7. In this work, we ignore defense mechanisms that cells possess against attack by methylglyoxal, other than DNA repair. Under exposure to MG, *E. coli* cells activate a detoxification pathway for the electrophile which triggers the acidification of the cytoplasm resulting in decreased toxicity of MG (33). *E. coli* strains used to perform the experiments presented in this work have genotype F^-, Δ*kdpABC5*, *thi*, *rha*, *lacZ*, *lacI*, *trkD1*, *gal*, *kefB*$^-$, *kefC*::Tn*10*, *gshA*::Tn*10* and therefore lack both the main detoxification pathway and the acidification mechanisms (see Experimental Protocols, below). We can then assume that the concentration and toxicity of MG are constant (see the Supporting Material).

Model construction

We formulate a mathematical model based on the assumptions laid out above. In the case of *E. coli* cells under MG stress, on which we shall focus from now on, the guanine bases are most relevant, because the others are not strongly affected by MG. Each guanine base in the chromosome can be in one of three states: undamaged (or normal), damaged (after reacting with methylglyoxal), and under repair (after a repair enzyme binds to the damaged base; see Fig. 1). A given base can undergo the following transformations:

1. A normal base can be damaged by MG, with a rate R_1 proportional to the concentration M of MG.
2. A repair enzyme can bind to a damaged site, with rate R_2; if this base is within a distance of L elements of the sequence from another base under repair on the opposite strand, a double-strand break is caused.
3. A base under repair is repaired in an average time $1/\gamma$ (rate R_3), and the base returns to its normal, undamaged state.

Under the usual mass action law assumptions, the rates of these three processes are given by

$$R_1 = \alpha M n_N, \tag{1}$$

where α(molecule^{-1} s^{-1}) is the reaction rate between MG and the guanine bases;

$$R_2 = \beta n_D n_E, \tag{2}$$

where β(s^{-1}) is the affinity of repair enzymes for the damaged guanine bases; and

$$R_3 = \gamma n_R, \tag{3}$$

where γ(s^{-1}) is the frequency at which repair is completed.

The meaning of the parameters and variables in the equations above is summed up in Table 1. Let N_E be the total number of initiating repair

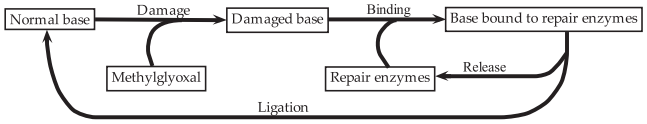

FIGURE 1 Flow chart of the dynamics of damage and repair of guanine bases under MG exposure. MG reacts with intact bases to form damaged bases; free repair enzymes bind to damaged bases and form a complex that releases a normal base and the repair enzyme once the repair is completed.

enzymes. Assuming that one enzyme molecule is used during each repair, we have the following conservation law:

$$N_E = n_E + n_R. \tag{4}$$

Analytic approach

In the analysis presented below, we assume that the concentration of the chemical damaging agent is constant over time. We have also studied the general case of decreasing MG, and the results are presented in the Supporting Material. If MG is constant, bases are damaged at a constant rate. These damaged bases are in turn eventually bound by repair enzymes, and then returned to the normal state when the repair is done. There is thus a constant flow from one state to the other. This flow is a cycle, driven by new damages caused by MG (see Fig. 1).

Of course this flow is not in reality a continuous process: each state transition of any given base is a stochastic event. But as a first approximation, we consider a deterministic, continuous flow, regarding the quantities n_N, n_D, n_R, and n_E as continuous variables. This allows us to use differential equations to describe the dynamics of these variables, which are more readily amenable to analytical approaches than the full-blown stochastic formulation. We will compare later this approximation with the full stochastic simulation, and find that the two approaches agree on their main predictions.

Using the continuous approximation, we write differential equations for the variables of the system:

$$\frac{dn_N}{dt} = R_3 - R_1, \tag{5}$$

TABLE 1 Definition of the parameters used in the model

Parameter	Definition
N_G	Total number of guanine bases.
N_E	Total number of repair enzymes.
n_N	Number of undamaged guanine bases.
n_D	Number of damaged guanine bases.
n_R	Number of guanine bases under repair (number of bound repair enzymes).
n_E	Number of free initiating repair enzymes.
M	Methylglyoxal concentration.
α	Constant measuring the reactivity of MG with guanine.
β	Constant measuring the affinity of the repair enzyme for a damaged guanine.
γ	Inverse of the average time it takes to complete a repair.
L	Number of bases removed during nucleotide excision repair.
$N_C = (\alpha/\gamma)\, N_G M$	Critical number of repair enzymes.
$R_1 = \alpha M n_n$	Rate of damage of normal bases.
$R_2 = \beta n_D n_E$	Rate of formation of complexes repair enzyme-damage.
$R_3 = \gamma n_R$	Rate at which repair finishes.

$$\frac{dn_D}{dt} = R_1 - R_2, \tag{6}$$

$$\frac{dn_R}{dt} = R_2 - R_3 = -\frac{dn_E}{dt}. \tag{7}$$

After MG is introduced in a bacterium's cytoplasm, a condition of steady state is quickly established, in which the flows from one state to the next are balanced. We find the steady-state number of bases in each state, and from this we calculate the probability that the next repair event will cause a double-strand break; this is proportional to the bound enzyme density N_R/N_G in steady state, where $N_G = n_N + n_D + n_R$ is the number of guanine bases in a strand, and is thus proportional to the chromosome size. We can also calculate the steady-state frequency with which repair enzymes bind to damaged sites. We define the half-life as the time at which the probability to create a double-strand break has reached 0.5. We can predict how it depends on the concentration of the damaging chemical and on the number of repair enzymes. This is done in Results, below.

Stochastic simulation

The approach described above could be criticized on the basis that some of the molecular numbers we are dealing with can be very small, notably the number of repair enzymes. In that case, the suitability of differential equations to describe the dynamics of the system is debatable. For this reason we also did a full Monte Carlo stochastic simulation of the model, where each individual event is simulated according to its appropriate probability distribution, using a version of the Gillespie algorithm. Each chromosome was encoded by two arrays corresponding to the two strands in DNA. Each entry of the arrays represents a guanine base, and throughout the simulation we keep track of which state every guanine base is in—normal, damaged, or under repair. The time evolution of a given realization of the system is simulated by essentially the Gillespie algorithm, with the reactions being the transitions from one state to another as described above, and the propensities being given by Eqs. 5–7. The only difference with respect to the usual Gillespie algorithm is that we keep track of the individual states of all the bases in the two arrays, rather than just dealing with the total number of bases in the different states, as would be the procedure in the normal Gillespie algorithm.

To predict the death rate, we insert an additional step in the simulation, in which we check at the beginning of every new repair if there is another base being repaired in the other strand within the "fatal distance" $L > 0$, which corresponds to the number of bases removed during excision repair. If so, we consider the cell to have died and stop the simulation. We record the time at which the cell dies and calculate the death rate as the inverse of this time.

The results from the stochastic simulations and from the analytical approach are compared and analyzed in the Discussion.

Experimental protocols

An *Escherichia coli* K-12 derivative strain, MJF335, was used in this study. Its genotype description is F$^-$, Δ*kdpABC5*, *thi*, *rha*, *lacZ*, *lacI*, *trkD1*, *gal*, *kefB*$^-$, *kefC*::Tn*10*, *gshA*::Tn*10*. It lacks the major glutathione-dependent detoxification pathway and protection mechanisms against methylglyoxal (no KefB/KefC to acidify the cytoplasm). The strain was cultured on solid Luria Bertani media and stored at 4°C for a maximum of three weeks. MJF335 was taken from the laboratory long-term stocks which were maintained in Protect Vials (Technical Service Consultants, Heywood, Lancashire) at −80°C.

Laboratory reagents were supplied by Fisher Scientific UK (Loughborough, Leicester), Sigma-Aldrich (Poole, Dorset), or BDH Supplies (Poole, Dorset). Tryptone, yeast extract, and agar (Technical Agar No. 3) were supplied by Oxoid (Basingstoke, Hampshire). MG was purchased from Sigma-Aldrich. The concentration of the MG stock solution was 5.6 M.

Cells were grown at 37°C and 300 rpm in 10 mL K120 medium (34) in a shaking incubator (Model G25; New Brunswick Scientific, Edison, NJ). To obtain exponentially growing cultures, cultures were diluted into fresh prewarmed growth medium to achieve an optical density at a wavelength of 650 nm (OD_{650}) of 0.05. The cells were grown to an OD_{650} of ≈0.4, diluted to an $OD_{650} = 0.05$ again into fresh media for another cycle. Once it reached an $OD_{650} = 0.4$, the midexponential cultures were then diluted into fresh prewarmed growth medium to an $OD_{650} = 0.04$.

Bacterial growth was determined by removing 1 mL aliquots of the culture into a disposable 1.5 mL cuvette. The OD was measured at a wavelength of 650 nm in a Novaspec II spectrophotometer (Pharmacia Biotech, Piscataway, NJ) at regular time intervals. The blank was set using the appropriate growth medium.

Cells were grown and diluted as described above. MG was added to achieve a concentration of 0.3 mM, 0.5 mM, 0.7 mM, and 0.9 mM. At intervals of 5 min, 20 μL aliquots were taken in duplicates and diluted into 180 μL K120 buffer in a 96-well plate. Using a multichannel pipette to handle all samples simultaneously, the diluted cells were mixed by up- and downpipetting and then serially diluted (10^{-1}–10^{-5}). New tips were used after each dilution step to avoid carry-over.

Cell viability was determined by spotting 20 μL aliquots of each dilution in four replicates on solid Luria Bertani plates. The plates were incubated overnight. The number of colony-forming units (CFU) were counted and the CFU/mL was calculated.

RESULTS

Analytical results

Equations 5–7 can be solved for the steady state, by setting all time derivatives to zero. In realistic conditions, the number of repair enzyme molecules and the total number of damaged bases at any time are both expected to be much smaller than the total number N_G of guanine bases. In this case, we can consider n_N (total number of normal bases) to be constant, with $n_N \approx N_G$. Using this approximation, the steady-state values of n_D (number of damaged bases), n_R (number of repair complexes), and n_E (number of free repair enzymes) are

$$n_R^0 = \frac{\alpha N_G M}{\gamma} = N_E - n_E^0, \tag{8}$$

$$n_D^0 = \frac{\alpha N_G M}{\beta\left(N_E - \frac{\alpha N_G M}{\gamma}\right)}. \tag{9}$$

The first point to note is that n_R^0 is proportional to the methylglyoxal concentration M. However, note that n_D^0 is positive only for values of $N_E > N_c$, where

$$N_c = n_R^0 = \frac{\alpha}{\gamma} N_G M. \tag{10}$$

In this case, the steady state is always stable. For values of N_E less than the critical value N_C, the steady state becomes negative and unstable and the number of damaged bases n_d increases with time without bound, whereas the number of repair complexes n_R equals N_E (see the Supporting Material and the Appendix). Thus N_c is a critical value which separates two different dynamical regimes of the system. We will assume for now that N_E is above N_c; we will argue later that this is the most biologically plausible regime. The case $N_E < N_c$ will be discussed later.

Our main goal is to calculate the rate of creation of DSB from this model. Let us define the half-life T to be the time it takes for half of the cells in a population to form a DSB. Alternatively, we can think of T as the time at which the probability P that a DSB appears in a single cell reaches the value 1/2. The death rate is defined as $1/T$. T can be calculated from two quantities: the probability p that the next repair to initiate will kill the cell, because it happens to be too close to another repairing site; and the average time interval Δt between two consecutive repair initiations.

From Eq. 6, in the steady state we get

$$\Delta t = (\beta n_D n_E)^{-1} = (\alpha N_G M)^{-1}.$$

To calculate p, consider the repairs which are going on in the chromosome immediately before a new repair is initiated. There is an interval of bases containing each of these repair sites, such that if the new repair initiates within one of these intervals on the opposite strand, a double-strand break appears and death ensues. Because we assume the number of repair enzymes to be much smaller than the chromosome size, these death intervals occupy only a small fraction of the total chromosome length, and are thus unlikely to overlap. This means that the total length covered by these intervals is to a good approximation $n_R L$, where L is the length of each interval. Hence, the probability p that the next repair is initiated within one of these intervals on the strand opposite to the preexisting repair is

$$p = \frac{L n_R}{2N_G}.$$

The factor 2 in the denominator arises because the two damages must be on opposite strands for a DSB to be formed. We assume here that all lesions are repaired by excision repair, although it is possible that some of them are repaired by homologous repair. We describe in the Supporting Material a modified version of the model which takes this fact into account; however, the results are not changed quantitatively, and the dependency of the half-life on the concentration of MG and other parameters is the same as discussed below (see the Supporting Material).

The half-life T is given by $n_{1/2}\Delta t$, where $n_{1/2}$ is the number of successively initiated repairs so that the DSB creation probability drops to 1/2:

$$(1-p)^{n_{1/2}} = 1/2.$$

Because we assume $N_E >> N_G$, we have $p << 1$. Using this fact, we get

$$n_{1/2} \approx \frac{\ln 2}{p}.$$

Putting all this together, we get for the half-life:

$$T = \frac{2\gamma \ln 2}{\alpha^2 L} N_G^{-1} M^{-2}. \quad (11)$$

The model therefore predicts that the population decays exponentially, with a half-life which is inversely proportional to the square of the concentration M of the damaging chemical. Note that it also predicts that the death rate does not depend on the number N_E of repair enzymes, as long as N_E is greater than N_c. This apparently counterintuitive result will be discussed at length in the Discussion. Also notice that these conclusions, as well as others to be discussed later on, do not depend on the precise values of the constants L, α, and γ.

In the derivation above, we assumed that the number of repair enzymes is $>N_c$, in which case the steady-state solution is stable. In this regime, the number of repair enzymes is enough to repair damaged bases at the same rate with which they are created by MG, and thus ensure that a steady-state condition sets in and that the number of damaged bases does not increase without bounds. If $N_E < N_c$, the steady-state solution of Eqs. 5–7 becomes negative and unstable (see the Supporting Material), and the number of damaged bases n_D increases continually. From Eq. 2, the binding rate of repair enzymes is proportional to the number of damaged sites n_D. As n_D increases, more and more repair enzymes are busy repairing the damaged sites, and after a time long enough, practically all N_E repair enzymes will be bound to damaged sites. So in this limit, we can use the approximation $n_R \approx N_G$. The system of Eqs. 5–7 can be analyzed in this limit, and the expression for the half-life in this regime (which we will call T^* to prevent confusion with Eq. 11) can be derived (see the Appendix for the derivation):

$$T^* = \frac{2\ln 2}{\gamma L} \frac{N_G}{N_E^2}. \quad (12)$$

The half-life in this regime has a very different dependence on MG concentration and on N_E, compared to that of the regime $N_E > N_c$. In particular, T^* does not depend on the MG concentration. Another counterintuitive result is that T^* decreases as the number of repair enzymes increases. These results, as well as some properties of T discussed in the previous paragraphs, may be very surprising at first. But as we will see in the Discussion, they have simple and intuitive interpretations, and arise from the subtle properties of the dynamics governing the processes of DNA damage and repair. For now we just remark that these results only appear counterintuitive if one thinks of death as arising directly from the damaged bases; but in reality the cause of death is intimately connected to the repair process, and this makes the relations among damage, repair, and death far from straightforward.

Stochastic simulation

Because the number of repair enzyme molecules in any given cell is low, it is prudent to verify the predictions of our model using a full-blown stochastic simulation, which does not assume n_D or n_R to be small, and takes into account the fact that they are discrete quantities with stochastic variations. The stochastic simulation scheme we developed is a variant of the Gillespie algorithm, and is explained in detail in Methods. The main results of the simulation are summarized in Fig. 2, *A* and *B*.

Fig. 2, *A* and *B*, shows the death rate as calculated from the model as a function of the MG concentration and the chromosome size, respectively, for

$$\alpha = 10^{-8}(\text{molecule} \cdot \text{s})^{-1}, \beta = 0.9\ \text{s}^{-1}, \text{and } \gamma = 1.6\ \text{s}^{-1}.$$

As discussed previously, the quadratic dependence of the death rate on MG concentration and the other main results do not depend on these values. The circles are the results of the simulation, and the solid line shows the fit to the equation $T^{-1} = a \cdot X^b$, and we find $b = 2.13$ for $X = \text{MG}$ and $b = 0.94$ for $X = N_G$. The stochastic simulations confirm that the death rate depends quadratically on MG concentration and linearly on the DNA size, as long as the MG concentration is not too low, and as long as N_G is not too small. The reason for the discrepancy between the two predictions in the low M and the small N_G limits is easily understood: in both these limits, the average number of repairing sites n_R is small, and the discrete nature of n_R and its stochastic fluctuations become important.

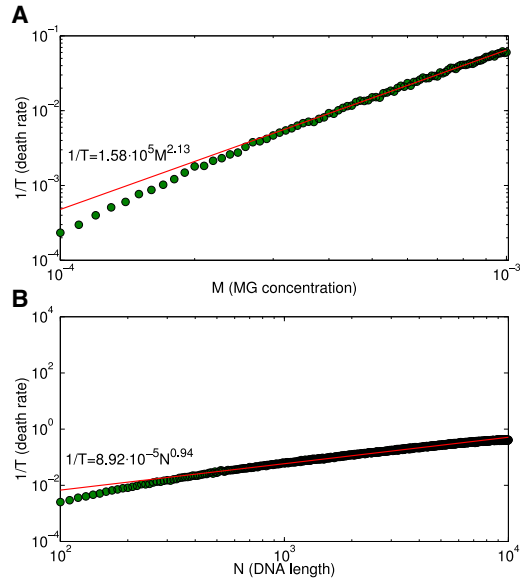

FIGURE 2 Dependency of the death rate on MG and N_G as predicted by the stochastic simulations; parameters were $\alpha = 10^{-8}$ molecule^{-1} s^{-1}, $\beta = 0.9\ \text{s}^{-1}$, $\gamma = 1.6\ \text{s}^{-1}$, $N_E = 50$, and $L = 6$ bases. (*A*) Death rate as a function of the MG concentration, MG $\in$ [0.1, 1] mM, $N_G = 2000$ bases. (*B*) Death rate as a function of the chromosome size, MG = 1 mM, $N_G \in$ [100, 10,000] bases. The MG concentration was converted in number of molecules of MG using a cell volume of 7.10^{-16} L (37) and the Avogadro number $N_A = 6.02 \times 10^{23}$. Shown are the results of the stochastic model (*green dots*), and the fit to the equation $T^{-1} = aX^b$ (*red lines*).

Experimental results

We performed experiments where *E. coli* cells were exposed to different concentrations of methylglyoxal, and the fraction of living cells was measured at different time points (see Fig. 3 *A*). Cells were considered to be alive if they were able to divide and form colonies. In wild-type *E. coli*, protective mechanisms in addition to the basic DNA repair process are triggered by the presence of MG: a detoxification pathway becomes active, which gradually degrades MG; this pathway is in turn coupled to the activation of a potassium efflux system (KefGB and KefFC) which causes a drop in the intracellular pH, which decreases the toxicity of MG (33). To isolate the effect of DNA repair, we used mutant strains in which the genes responsible for the MG detoxification pathway and the ion channel were knocked out (see details in Methods).

Fig. 3 *A* shows the change in the fraction of living cells with time, for different MG concentrations ranging from 0.3 mM to 0.9 mM. It has been shown (20) that cell viability decreases above 0.6 mM of MG, whereas there is no net cell growth above 0.3 mM MG, suggesting that for concentrations above 0.3 mM individual cells have stopped growing. Therefore we can safely assume that a decrease in numbers of viable cells is caused solely by cell death, and that replication is halted. From these curves, we can calculate the death rate for each concentration; this is plotted in Fig. 3 *B*. First notice that the death rate depends strongly on M, which indicates that we are in the regime where $N_E > N_c$, and the steady-state assumption should hold. Equation 11 predicts then that the points in Fig. 3 *B* should lie on a straight line, with slope 2, as indicated by the solid line in the figure. Although the experimental errors are large, the figure shows that the results agree reasonably well with our theoretical prediction, if we identify double-strand break formation with cellular death.

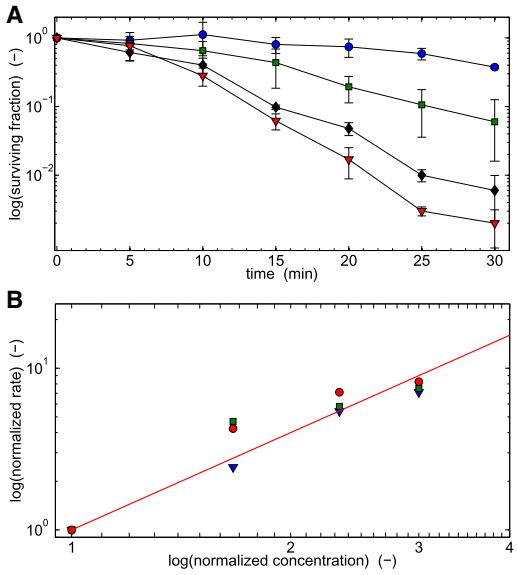

FIGURE 3 Experimental measurements of the dynamics of cell death under exposure to MG. (*A*) Time course of the fraction of living cells, for different concentrations of MG: 0.3 mM (*blue circles*), 0.5 mM (*green squares*), 0.7 mM (*black diamonds*), and 0.9 mM (*red crosses*). (*B*) Measured death rate as a function of MG concentration; three different repeats of the experiment are shown.

DISCUSSION

It may be surprising at first that the expression for the half-life T (Eq. 11) does not depend on the total number of repair enzymes. Of course, Eq. 11 was derived assuming that $N_E > N_c$, but as long as N_E remains above N_c, the prediction is that changes in N_E do not affect the death rate. The reason for this is that the death rate does not arise directly from the damage; it is instead a result of the repair process itself (8,9,24). The DSB creation rate is determined by the number n_R of repair processes taking place in the chromosome; and in steady-state conditions this number, as can be seen from Eq. 8, is independent of N_E in the steady-state regime.

If the number of repair enzymes is large enough to repair damaged sites with the same rate they are created (that is, if $N_E > N_c$), any further increase in N_E will not result in more repairs, because only damaged bases can be repaired, and they are created with a rate fixed by the MG concentration. The independence of n_R with respect to N_E was verified by the direct stochastic simulation. The result is shown in Fig. 4, which plots the average value of n_R as a function of N_E. We see that as soon as N_E becomes greater than $N_c \approx 3$, n_R settles to a constant value, as predicted by Eq. 8.

The quadratic dependence of the death rate on the MG concentration M has a simple interpretation. An increase in M results in a proportional increase in the "death probability" p, because from Eq. 8 the density n_R/N_G of repair sites is proportional to M. An increase in M also results in the proportional decrease of the average time $\Delta t = (\gamma\, n_R^0)^{-1}$ between two consecutive repair initiations, because there are more MG molecules which can cause damage; this in turn increases the death rate in the same proportion.

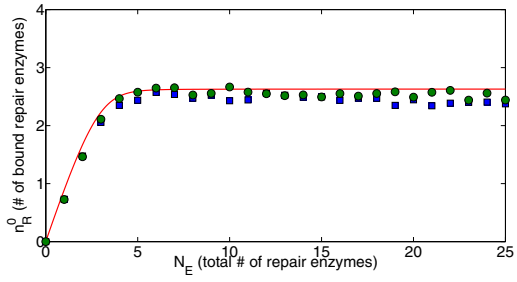

FIGURE 4 Stationary number of bases under repair, n_R, as a function of total number of repair enzymes N_E. Parameters used in the simulation were $\alpha = 10^{-8}$ molecule^{-1} s^{-1}, $\beta = 0.9$ s^{-1}, $\gamma = 1.6$ s^{-1}, $N_G = 2000$ bases, $M = 0.5$ mM, and $N_E \in [0, 25]$; the critical number of repair enzymes is $N_C = 2.6$. Shown are two stochastic simulations (*green circles* and *blues squares*) and the result from the deterministic equations (*red line*).

These two factors—the increase in p and the decrease in Δt—contribute each with a power of M to the death rate, resulting in the quadratic dependence of Eq. 11. The death rate is also quadratically dependent on the reactivity α of MG with guanine bases; this can be understood in the same way as the MG dependence explained above. This result implies that the decrease in the reactivity of the damaging chemical results in a very large decrease in the DSB creation rate and consequently on the death rate. This is consistent with the experimental observation that in wild-type *E. coli* cells, the toxicity of MG is decreased by acidification of the cytoplasmic pH after activation of the KefGB/KefFC systems during exposure to MG (18,35,36).

Equation 11 also predicts that the death rate is proportional to the chromosome size. An increase in N_G does not change the density n_R/N_G of damaged bases (see Eq. 8), and therefore has no effect on the probability p of double-strand break formation. But it does increase the number of sites under repair n_R^0, which decreases the interrepair interval Δt.

It should be stressed here that these conclusions are only valid as long as $N_E > N_c$. For example, if M is increased, so does

$$N_c = \frac{\alpha}{\gamma} N_G \times M.$$

As long as N_E remains greater than N_c, the quadratic dependence predicted by Eq. 11 holds; but if M increases so much that N_c becomes greater than N_E, Eq. 11 is no longer true.

In the $N_E < N_c$ case, the half-life is given by Eq. 12, which predicts that the death rate does not depend on the concentration of MG, which may seem quite strange. The key to understanding this is again the fact that death rate is not determined by the number of damaged bases, which in this regime keeps increasing; the death rate is governed by the number of repairs n_R, and this has a maximum value of N_E, regardless of how high M may be. When n_R reaches its saturation value N_E, increases in the MG concentration have no effect on the rate of double-strand break formation, and hence on the death rate, because we are assuming death is caused only by double-strand breaks.

Contrary to most mathematical models of DNA damage-induced death, our model investigates the lethal potential of repair mechanisms, and we derive an explicit analytical expression for the death rate of the population. Very often, the decline in cell population is modeled as a first-order kinetics process, but no attempt is made to model the molecular mechanisms leading to death (12,13). The most widely used models belong to the generic class of multihit, multitarget models (14–17), which are based on the idea that death occurs when some defined critical targets (usually proteins and RNA) have been inactivated; the standard model among the radiation biology community is the linear quadratic model, which assumes that DNA double-strand breaks are directly caused by the threatening agents (11,16), in this case ionizing radiation. If repair is considered, it is usually assumed that it is always beneficial and results in reduced mortality—such as, for example, in models of ultraviolet radiation damage and repair by photoreactivation (14). Although under some conditions these assumptions may be justified, they do not hold for situations like the exposure of *E. coli* cells to MG, and we suspect the deleterious effects of DNA repair are important in many other systems.

In summary, we have constructed a minimal model of the dynamics of DNA damage and repair of single base damages. Even though the model we propose is idealized, it shows nevertheless that the relation between DNA damage and cell death is far from straightforward. The fact that repair can cause death is usually ignored or brushed aside by most existing models. However, we have shown that this effect leads to predictions which challenge commonly held assumptions about the processes of DNA damage and repair, and their relation to cell death.

APPENDIX: UNSTABLE REGIME, $N_E < N_C$

For $N_E < N_c$, the number of damages n_D increases indefinitely, which in turn increases the rate R_2 of enzyme-damage binding. Assuming that the binding constant β is not too small, for long enough times practically all repair N_E enzymes will be busy repairing damages, and we will have $n_R \approx N_E$, and consequently $dn_R/dt \approx 0$. Substituting this into Eq. 3, we get $\beta n_D n_E = \gamma N_E$. Using this in turn in Eq. 1, and assuming again $n_N \approx N_G$, we find

$$\frac{dn_D}{dt} = \alpha N_G M - \gamma N_E = constant,$$

and so n_D increases linearly in the asymptotic limit $t \to \infty$.

The probability p of a double-strand break forming when the next repair starts is in this limit

$$p = \frac{n_R L}{2N_G} = \frac{N_E L}{2N_G}. \quad \text{(A1)}$$

The interrepair interval Δt is given by $(\gamma n_R)^{-1}$, or

$$\Delta t = (\gamma N_E)^{-1}. \quad \text{(A2)}$$

The half-life T is given by

$$T = \frac{\ln 2}{p}\Delta t,$$

and substituting Eqs. A1 and A2, we get Eq. 12.

SUPPORTING MATERIAL

One figure and 14 equations are available at http://www.biophysj.org/biophysj/supplemental/S0006-3495(10)05257-4.

This work was supported by the British Biotechnology and Biological Sciences Research Council (grant No. BB/F003455/1, SysMo initiative).

REFERENCES

1. Kuzminov, A., and F. Stahl. 2004. Overview of homologous recombination and repair machines. *In* The Bacterial Chromosome. P. Higgins, editor. American Society for Microbiology, Washington, DC. 349–367.
2. Ferguson, G. P., S. Tötemeyer, …, I. R. Booth. 1998. Methylglyoxal production in bacteria: suicide or survival? *Arch. Microbiol.* 170:209–218.
3. Sedgwick, S. G., C. Ho, and R. Woodgate. 1991. Mutagenic DNA repair in enterobacteria. *J. Bacteriol.* 173:5604–5611.
4. Kreuzer, K. N. 2005. Interplay between DNA replication and recombination in prokaryotes. *Annu. Rev. Microbiol.* 59:43–67.
5. Strauss, B. 2004. Excision repair and bypass. *In* The Bacterial Chromosome. P. Higgins, editor. American Society for Microbiology, Washington, DC. 431–447.
6. Sancar, A. 1996. DNA excision repair. *Annu. Rev. Biochem.* 65:43–81.
7. Moss, S. H., and D. J. G. Davies. 1974. Interrelationship of repair mechanisms in ultraviolet-irradiated Escherichia coli. *J. Bacteriol.* 120:15–23.
8. Pennington, J. M., and S. M. Rosenberg. 2007. Spontaneous DNA breakage in single living *Escherichia coli* cells. *Nat. Genet.* 39: 797–802.
9. Michel, B., S. D. Ehrlich, and M. Uzest. 1997. DNA double-strand breaks caused by replication arrest. *EMBO J.* 16:430–438.
10. Krasin, F., and F. Hutchinson. 1977. Repair of DNA double-strand breaks in *Escherichia coli*, which requires recA function and the presence of a duplicate genome. *J. Mol. Biol.* 116:81–98.
11. Chadwick, K. H., and H. P. Leenhouts. 2005. Radiation risk is linear with dose at low doses. *Br. J. Radiol.* 78:8–10.
12. Hunt, D. E., and R. F. Pittillo. 1967. Killing of cells in bacterial colonies. *Appl. Microbiol.* 15:334–339.
13. Lambert, R. J. W., and M. D. Johnston. 2000. Disinfection kinetics: a new hypothesis and model for the tailing of log-survivor/time curves. *J. Appl. Microbiol.* 88:907–913.
14. Beggs, C. B. 2002. A quantitative method for evaluating the photoreactivation of ultraviolet damaged microorganisms. *Photochem. Photobiol. Sci.* 1:431–437.
15. Miles, C. A. 2006. Relating cell killing to inactivation of critical components. *Appl. Environ. Microbiol.* 72:914–917.
16. Steel, G. G. 1993. Basic Clinical Radiobiology. Hodder-Arnold, London, UK.
17. Klotz, B., D. L. Pyle, and B. M. Mackey. 2007. New mathematical modeling approach for predicting microbial inactivation by high hydrostatic pressure. *Appl. Environ. Microbiol.* 73:2468–2478.
18. Ferguson, G. P., J. R. Battista, …, I. R. Booth. 2000. Protection of the DNA during the exposure of *Escherichia coli* cells to a toxic metabolite: the role of the KefB and KefC potassium channels. *Mol. Microbiol.* 35:113–122.
19. Booth, I. R., G. P. Ferguson, …, S. Kinghorn. 2003. Bacterial production of methylglyoxal: a survival strategy or death by misadventure? *Biochem. Soc. Trans.* 31:1406–1408.
20. Tötemeyer, S., N. A. Booth, …, I. R. Booth. 1998. From famine to feast: the role of methylglyoxal production in *Escherichia coli*. *Mol. Microbiol.* 27:553–562.
21. Krymkiewicz, N. 1973. Reactions of methylglyoxal with nucleic acids. *FEBS Lett.* 29:51–54.
22. Kell, D. B., A. S. Kaprelyants, …, M. R. Barer. 1998. Viability and activity in readily culturable bacteria: a review and discussion of the practical issues. *Antonie van Leeuwenhoek.* 73:169–187.
23. Niven, G. W., J. S. Morton, …, B. M. Mackey. 2008. Influence of environmental stress on distributions of times to first division in *Escherichia coli* populations, as determined by digital-image analysis of individual cells. *Appl. Environ. Microbiol.* 74:3757–3763.
24. Haefner, K. 1968. Spontaneous lethal sectoring, a further feature of *Escherichia coli* strains deficient in the function of rec and uvr genes. *J. Bacteriol.* 96:652–659.
25. Gunderson, C. W., and A. M. Segall. 2006. DNA repair, a novel antibacterial target: Holliday junction-trapping peptides induce DNA damage and chromosome segregation defects. *Mol. Microbiol.* 59:1129–1148.
26. Woodgate, R., and D. G. Ennis. 1991. Levels of chromosomally encoded Umu proteins and requirements for in vivo UmuD cleavage. *Mol. Gen. Genet.* 229:10–16.
27. Bridges, B. A. 1980. Induction of enzymes involved in DNA repair and mutagenesis. *In* Environmental Chemicals, Enzyme Function and Human Disease. D. Evered and G. Lawrenson, editors. Elsevier Science, Dordrecht, The Netherlands. 67–82.
28. Kenyon, C. J., and G. C. Walker. 1980. DNA-damaging agents stimulate gene expression at specific loci in *Escherichia coli*. *Proc. Natl. Acad. Sci. USA.* 77:2819–2823.
29. Bridges, B. A., and R. P. Mottershead. 1978. Mutagenic DNA repair in *Escherichia coli*. VII. Constitutive and inducible manifestations. *Mutat. Res.* 52:151–159.
30. Jeggo, P., T. M. Defais, …, P. Schendel. 1977. An adaptive response of *E. coli* to low levels of alkylating agent: comparison with previously characterized DNA repair pathways. *Mol. Gen. Genet.* 157:1–9.
31. Sedgwick, S. G. 1975. Inducible error-prone repair in *Escherichia coli*. *Proc. Natl. Acad. Sci. USA.* 72:2753–2757.
32. Frischmann, M., C. Bidmon, …, M. Pischetsrieder. 2005. Identification of DNA adducts of methylglyoxal. *Chem. Res. Toxicol.* 18:1586–1592.
33. Ferguson, G. P. 1999. Protective mechanisms against toxic electrophiles in *Escherichia coli*. *Trends Microbiol.* 7:242–247.
34. Epstein, W., and B. S. Kim. 1971. Potassium transport loci in *Escherichia coli* K-12. *J. Bacteriol.* 108:639–644.
35. Ferguson, G. P., A. W. Munro, …, I. R. Booth. 1993. Activation of potassium channels during metabolite detoxification in *Escherichia coli*. *Mol. Microbiol.* 9:1297–1303.
36. MacLean, M. J., L. S. Ness, …, I. R. Booth. 1998. The role of glyoxalase I in the detoxification of methylglyoxal and in the activation of the KefB K^+ efflux system in *Escherichia coli*. *Mol. Microbiol.* 27:563–571.
37. Sundararaj, S., A. Guo, …, D. S. Wishart. 2004. The CyberCell Database (CCDB): a comprehensive, self-updating, relational database to coordinate and facilitate in silico modeling of *Escherichia coli*. *Nucleic Acids Res.* 32(Database issue):D293–D295.